Journal of Materials Chemistry A

Accepted Manuscript

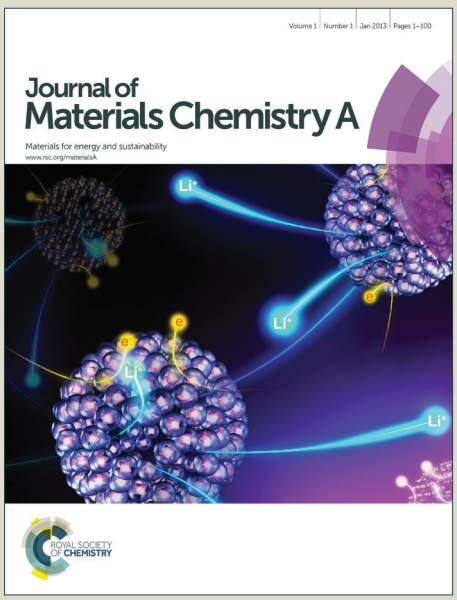

ROYAL SOCIETY OF CHEMISTRY

www.rsc.org/materialsA

Journal Name

RSCPublishing

ARTICLE

Tailoring the Water Adsorption Properties of MIL-101 Metal-Organic Frameworks by Partial Functionalization

Cite this: DOI: 10.1039/xoxxoooooox

Received ooth January 2012,
Accepted ooth January 2012

DOI: 10.1039/xoxxoooooox

www.rsc.org/

Nakeun Ko,[a] Pan Gyu Choi,[a] Jisu Hong,[a] Miso Yeo,[a] Siyoung Sung,[a,]* Kyle E. Cordova,[b] Hye Jeong Park,[a] Jin Kuk Yang,[a,]* and Jaheon Kim [a,]*

MIL-101 and MIL-101-NH_2 were partially modified to incorporate various functional groups that are capable of forming hydrogen bonds with water. Specifically, MIL-101-NH_2 was partially functionalized with $–NHCONHCH_2CH_3$ (–UR2), –NHCOCHCHCOOH (–Mal), or $–NH(CH_2)_3SO_3H$ ($–3SO_3H$) and MIL-101 was partially functionalized with –COOH in order to investigate the effect of these groups on the water sorption properties when compared to the pristine versions. The MIL-101 derivatives were synthesized by either post-synthetic modification of MIL-101-NH_2 or through direct synthesis using a mixed linker strategy. The ratios of the incorporated functional groups were determined by ^{1}H-NMR analyses and the porosity changes were revealed by N_2 gas adsorption measurements at 77 K. Water sorption isotherms at 298 K conclude that the incorporation of $–3SO_3H$ enhances the water vapour uptake capacity at a low relative pressure ($P/P_0 = 0.30$), whereas –UR2 and –Mal retard water adsorption in MIL-101-NH_2. The partial incorporation of –COOH in MIL-101 exhibits a steeper water uptake at lower pressure ($P/P_0 = 0.40$) than MIL-101-NH_2. Interestingly, a greater –COOH content within the MIL-101 framework reduces the water uptake capacity. These results indicate that even partial functionalization of MIL-101 induces noticeably large changes in the water adsorption properties.

Introduction

Reversible adsorption and desorption of water vapour in solid materials can be applied for air dehumidification,[1] delivery of fresh water in remote areas,[2] and heat transformations for cooling and heating.[3] In particular, adsorptive heat transformation (AHT) applications, such as thermally driven adsorption chillers or adsorption heat pumps, utilize heat transformation via adsorption/desorption of water vapour by solid materials and are considered to be highly energy-efficient and environmentally friendly technologies.[3] A general working cycle of AHT is initiated by evaporation of a working fluid, such as water, and then adsorption by a solid, porous material at ~25 °C. Evaporation of the working fluid results in useful cold fluid in the external surroundings serving as a chiller. When a solid material adsorbs the evaporating water, heat is released into the external surroundings, therefore, working as a heat pump. For the regeneration of the adsorbent material, solar thermal energy or low temperature waste heat at ~80 °C is then applied.[3d] Since AHT can be operated by inexpensive energy sources, consumption of electric power can be reduced. Indeed it is true that water sorbent materials will increasingly save more energy, which has led to significant research efforts being devoted to developing new materials whose water uptake capacity exceeds commercialized materials for these applications, such as SAPO-34 and regular density silica.[3d,4]

Metal-organic frameworks (MOFs), a class of crystalline, porous materials, are considered to be promising water sorbent candidates due to their large water uptake capacity.[3a-c] While most MOFs have low water stability,[3c] several reported structures were shown to be quite durable in water with their uptake capacity decreasing only slightly after repeated water sorption cycles.[3b] Typically, water adsorption in these frameworks begins at hydrophilic sites near metal centres, and then propagate to the hydrophobic organic linkers as pressure increases.[3c] Furthermore, the relative pressure, $\alpha = P/P_0$, "at which half of the total water capacity is reached" tends to decrease when organic linkers are functionalized with hydrophilic groups, leading to an increase in the Henry constants and a decrease in the pore filling pressure.[5] It is also reported that the pore filling process is continuous and reversible below a critical diameter ($D_c \sim 20$ Å) for rigid frameworks.[5] These findings and observations must be taken into consideration when developing MOFs that adsorb water steeply within a requested low pressure range of $0.05 < P/P_0 < 0.40$ necessary for effective AHT processes.[3a-d] Indeed, a steep and "S"-shaped water adsorption isotherm in this narrow pressure range results in two beneficial properties: the efficient

usage of energy (waste heat) and a large water uptake that correlates with a large working capacity of the employed water sorbent.

In general, the introduction of hydrophilic functional groups to the organic linker is considered to be a rational approach for enhancing water adsorption at lower pressures. Thus far, functionalization of MOF linkers with $–NH_2$ groups has proven most successful in shifting the isotherms of pristine, un-functionalized MOFs to lower pressure regions as demonstrated in Cr-MIL-101-NH_2,[6] Ga-MIL-53-NH_2,[5] and Ti-MIL-125-NH_2.[5,7] However, the $–NH_2$ functionalization strategy is not an effective solution for all MOFs. In CAU-10-X MOFs, the steep water uptake at $P/P_0 = 0.1 – 0.2$ for X = –H disappears when X = $–NH_2$ is introduced. This observation is most likely due to changes in the pore environment resulting from smaller pore sizes.[8] Similar to CAU-10-H, an un-functionalized framework itself can display desirable water uptake properties. In the case of MOF-841, there is a significant uptake accompanied by a nearly reversible, steep adsorption and desorption of water at $0.20 < P/P_0 < 0.30$.[1c] Nevertheless, it remains a significant challenge to directly synthesize new MOFs with impressive water uptake properties as the prediction of water adsorption isotherms for target materials is not abundantly straightforward. In this regard, the introduction of hydrophilic groups within known MOF frameworks and the subsequent investigations of their effects on the water sorption properties is a necessary strategy for realizing MOFs as water sorbents for AHT processes.

Cr-MIL-101, or simply MIL-101,[9] is composed of Cr_3O^{7+} clusters and 1,4-benzenedicarboxylate (BDC) linkers as shown in Fig. 1. MIL-101 has a proven water stability and large water uptake capacity ($1.0 – 1.4$ g g^{-1} at $P/P_0 = 0.9$).[3c,6,10,11] The large windows and pores of this MOF provide opportunities for introducing various functionalities covalently to its BDC linkers via pre- or post-synthetic modification methods (Scheme 1). Accordingly, MIL-101 is a suitable system to correlate in a systematic way the relationship between introduced functional groups and their effect on the water adsorption behaviours of the sorbent material. Previous reports reveal that the water adsorption isotherms of MIL-101, functionalized with $–NO_2$, $–SO_3H$, or $–NH_2$ groups, were significantly altered as a result of the hydrophilicity or hydrophobicity of the incorporated functional groups.[3c,6] Interestingly, the improvement in the water adsorption properties of MIL-101 in the form of steep water uptake at a lower pressure range or with a smaller α value (0.36 – 0.42 for MIL-101-NH_2 *vs*. 0.42 – 0.46 for MIL-101),[3c] could be achieved by partial functionalization of the framework with $–NH_2$ (BDC : BDC-NH_2 = 0.22 : 0.78 in Cr-MIL-101-*p*NH_2, where *p* stands for partial functionalization).[6b] Moreover, the water uptake capacity of Cr-MIL-101-*p*NH_2 remained unchanged during cycling tests whereas the fully-functionalized MIL-101-NH_2 led to a fluctuated and reduced capacity. From these experimental observations, we speculated that the water sorption behaviour of MIL-101 might be improved significantly by partial functionalization with other hydrophilic groups. Upon closer examination of the fully functionalized MIL-101-NH_2, there is a high probability that 2 faces in one super-tetrahedron (ST) unit are functionalized with two $–NH_2$ groups, respectively. This is likely because there are 6 BDC edges and 4 trigonal faces per ST (Fig. 1). Therefore, a partial replacement of these two $–NH_2$ groups with other functional groups can afford two different surface structures, which will influence the water affinity properties of the overall frameworks. However, it is noted that in reality, the structure will exhibit a more complex heterogeneity.

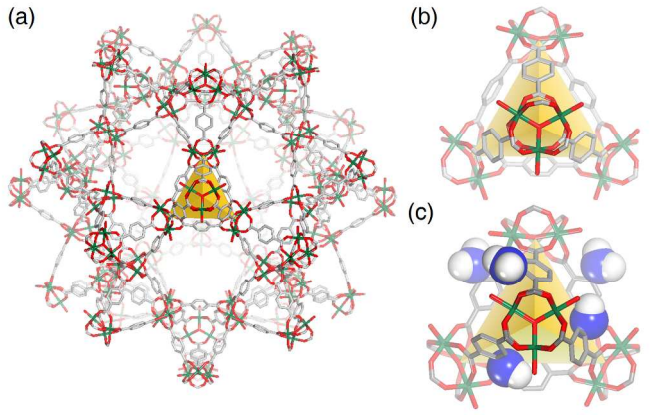

Fig. 1 (a) Crystal structure of MIL-101 demonstrated by a large (3.4 nm) cage with a highlighted super-tetrahedron (ST) as a structural building unit. (b) A ST in MIL-101 shown with stick models. (c) A ST in MIL-101-NH_2 with space filling $–NH_2$ groups displayed. Note the $–NH_2$ groups located on the ST faces. Colour codes: C, grey; H, white; N, blue; O, red; Cr, dark green. All H atoms except for those in $–NH_2$ groups are omitted for clarity. The STs are geometry-optimized models.

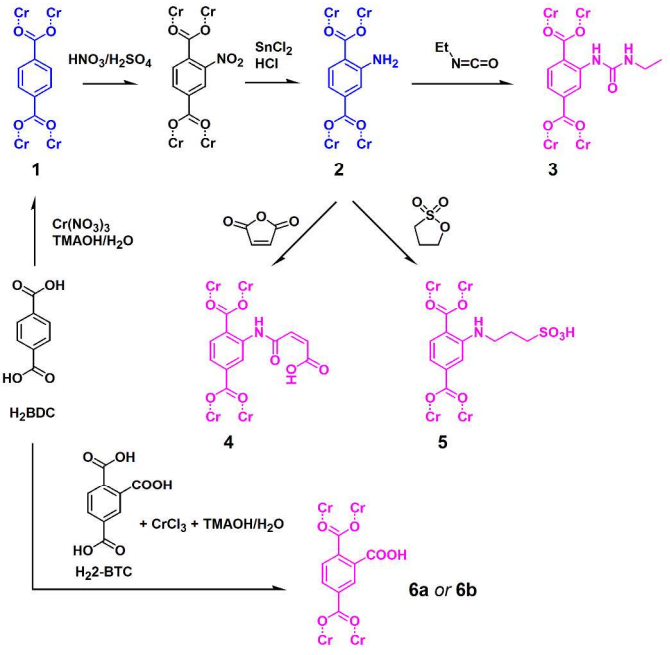

Scheme 1 The preparations of MIL-101 and its derivatives in this work are schematically drawn. MIL-101 derivatives containing two kinds of functional groups in the framework are highlighted with pink colour. TMAOH stands for tetramethylammonium hydroxide.

In this work, we have investigated the water adsorption properties of a series of partially functionalized MIL-101 derivatives and compared them with those of un-functionalized MIL-101 (**1**) or fully functionalized MIL-101-NH_2 (**2**) (Fig. 1). Hydrophilic groups (–$NHCONHCH_2CH_3$ (–UR2), –NHCOCHCHCOOH (–Mal), –$NH(CH_2)_3SO_3H$ (–$3SO_3H$), and –COOH) that are capable of forming hydrogen bonds with water were selected and partially incorporated within MIL-101 or MIL-101-NH_2. Accordingly, the resulting MIL-101-*p*UR2 (**3**), MIL-101-*p*Mal (**4**) and MIL-101-*p*$3SO_3H$ (**5**) were prepared via post-synthetic modification of MIL-101-NH_2, while MIL-101-*p*COOH (**6**) was directly prepared by using a mixed linker strategy that combined H_2BDC with $H_2$2-BTC (2-carboxy-benzene-1,4-dicarboxylic acid) during the synthesis (Scheme 1). Additionally, to further investigate the influence of 2-BTC in the framework, **6a** and **6b** were prepared using different ratios of these mixed linkers.

Experimental

Synthesis and characterization of MIL-101 structures

MIL-101 (**1**) and its derivatives were prepared according to reported methods with slight modifications made. For the preparations of MIL-101-NO_2, MIL-101-NH_2 (**2**), and MIL-101-*p*UR2 (**3**), sequential post-synthetic methods[12] were applied. MIL-101-*p*Mal (**4**) and MIL-101-*p*$3SO_3H$ (**5**) were obtained by applying the ring opening reactions used for the post-synthetic modification of IRMOF-3 with maleic anhydride[13] and 1,3-propanesultone.[14] The mixed-linker MIL-101-*p*COOH (**6**) was prepared according to the mixed-linker and high-throughput method.[15] The crystallinity and porosity changes were monitored by powder X-ray diffraction (PXRD) and N_2 adsorption measurements. The ratios of the organic linkers incorporated were identified by ^{1}H-NMR measurements on the respective digested MOF samples.

For ^{1}H-NMR measurements, MOF samples were appropriately treated to remove paramagnetic Cr ions.[6b,12,15] In a typical treatment, a sample (10 mg) was dissolved in an NMR solution prepared by mixing 40 wt% NaOD/D_2O (2.0 μL) and D_2O (1.0 mL). Upon dissolving the MOF crystals, chromium hydroxide precipitated. However, the solution's colour remained slightly greenish, indicating some Cr species were still present in the NMR solution. The solution was allowed to stand on a bench for additional 2 days in order to induce further precipitation of the chromium species. The precipitate was subsequently removed by centrifuge and filtration, and the filtrate was analysed by NMR.

MIL-101 (1). MIL-101 was synthesized according to the reported procedure with slight modifications.[16] A solid mixture of H_2BDC (3.32 g, 0.02 mol) and $Cr(NO_3)_3{\cdot}9H_2O$ (8.0 g, 0.02 mol) was suspended in a mixture of H_2O/TMAOH (100/1.8 mL) in a 300 mL hydrothermal Teflon vessel. The vessel was locked in a digestion bomb and heated in an isothermal oven at 180 °C for 24 h to yield green powder. The reaction mixture was allowed to cool naturally to room temperature and the powder was washed with copious amounts of deionized water, DMF, and EtOH. ^{1}H-NMR (NaOD/D_2O, 400 MHz): δ 7.88 (s, 4H) ppm.

MIL-101-NO_2. MIL-101 (500 mg) was soaked in a conc. HNO_3 (25 mL)/H_2SO_4 (35 mL) solution mixture in an ice bath and stirred for 15 minutes. The mixture was then removed and stirred overnight (> 12 h) at room temperature. After this, the solution was poured into crushed ice. The resulting green powder was collected and then washed with copious amounts of deionized water, DMF, and EtOH. ^{1}H-NMR (NaOD/D_2O, 400 MHz): δ = 8.51 (d, J = 1.6 Hz, 1H), 8.18 (dd, J = 7.6, 1.6 Hz, 1H), 7.55 (d, J = 8 Hz, 1H) ppm.

MIL-101-NH_2 (2). MIL-101-NO_2 (**1**) (500 mg) and $SnCl_2{\cdot}2H_2O$ (3.5 g) were added to a 250 mL round-bottom flask containing 150 mL of EtOH. The mixture was then refluxed for 12 h. After this, the mixture was allowed to cool to room temperature and conc. HCl (50 mL) was added and the resulting mixture was stirred for an additional 6 h. The solution was then poured into crushed ice. The resulting green powder was collected and washed with copious amounts of deionized water, DMF, and EtOH. ^{1}H-NMR (NaOD/D_2O, 400 MHz): δ = 7.70 (d, J = 8.0 Hz, 1H), 7.27 (d, J = 1.6 Hz, 1H), 7.20 (dd, J = 8.0, 1.6 Hz, 1H) ppm.

MIL-101-*p*UR2 (3). MIL-101-NH_2 (**2**) (200 mg) was placed in a 20 mL vial containing a mixture of Et-NCO (0.5 mL) and DMF (10 mL). The vial was then capped and heated in an isothermal oven at 120 °C for 24 h. The resulting solid product was washed with copious amounts of DMF and EtOH. ^{1}H-NMR (NaOD/D_2O, 400 MHz): δ = 8.35 (s, 1H), 7.83 (d, J = 8.4 Hz, 1H), 7.70 (d, J = 8.4 Hz, 1H), 7.49 (dd, J = 8.0, 1.6 Hz, 1H), 7.27 (d, J = 1.6 Hz, 1H), 7.20 (dd, J = 8.4, 1.6 Hz, 1H), 2.91 (q, J = 7.33 Hz, 2H), 1.19 (t, J = 7.4 Hz, 3H) ppm.

MIL-101-*p*Mal (4). MIL-101-NH_2 (**2**) (200 mg) was placed in a 20 mL vial containing a mixture of maleic anhydride (98 mg) and methylene chloride (10 mL). The vial was capped and kept at room temperature for 48 h. The resulting solid product was washed with copious amounts of methylene chloride and EtOH. ^{1}H-NMR (NaOD/D_2O, 400 MHz): δ = 8.66 (d, J = 9.6 Hz, 1H), 7.89 (d, J = 8.0 Hz, 1H), 7.70 (d, J = 8.0 Hz, 1H) 7.62 (dd, J = 8.4, 2.0 Hz, 1H), 7.27 (d, J = 2.0 Hz, 1H), 7.20 (dd, J = 8.0, 1.6 Hz, 1H), 6.50 (d, J = 12.4 Hz, 1H), 6.09 (d, J = 11.6 Hz, 1H) ppm.

MIL-101-*p*$3SO_3H$ (5). MIL-101-NH_2 (**2**) (130 mg) was placed in a 20 mL vial containing a mixture of 1,3-propanesultone (0.13 mL) and chloroform (10 mL). The vial was capped and heated in an isothermal oven at 45 °C for 24 h. The solid product was washed with copious amounts of chloroform and EtOH. ^{1}H-NMR (NaOD/D_2O, 400 MHz): δ = 7.77 (d, J = 8.4 Hz, 1H), 8.0 (d, J = 8.0 Hz, 1H), 7.30 (d, J = 1.6 Hz, 1H), 7.27 (d, J = 1.6 Hz, 1H), 7.20 (dd, J = 8.0, 2.0 Hz, 1H), 7.17 (dd, J = 8.0, 1.6 Hz, 1H), 3.37 (t, J = 7.0 Hz, 2H), 3.05 (t, J = 7.8 Hz, 2H), 2.10 (m, 2H) ppm.

MIL-101-*p*COOH (6). A solid mixture of H_2BDC (72.8 mg, 0.44 mmol for **6a**; 54.6 mg, 0.33 mmol for **6b**), $H_2$2-BTC (91.7 mg, 0.44 mmol for **6a**; 114.6 mg, 0.55 mmol for **6b**) and $CrCl_3$ (138.6 mg, 0.88 mmol) was dissolved in a mixture of H_2O/TMAOH (7.0/0.15 mL) in a 23 mL Teflon vessel. The vessel was locked in a digestion bomb and heated in an isothermal oven at 180 °C for 96 h to afford green powder. The collected powder was copiously washed

with DMF and EtOH. ^{1}H-NMR (NaOD/D_2O, 400 MHz) for **6a**: δ = 7.90 (s, 1H), 7.87 (s, 1H), 7.83 (d, J = 7.6 Hz, 1H), 7.47 (d, J = 8.0 Hz, 1H) ppm.; for **6b**: δ = 7.91 (d, J = 7.6 Hz, 1H), 7.87 (s, 1H), 7.83 (dd, J = 8.0, 1.6 Hz, 1H), 7.48 (d, J = 8.0 Hz, 1H) ppm.

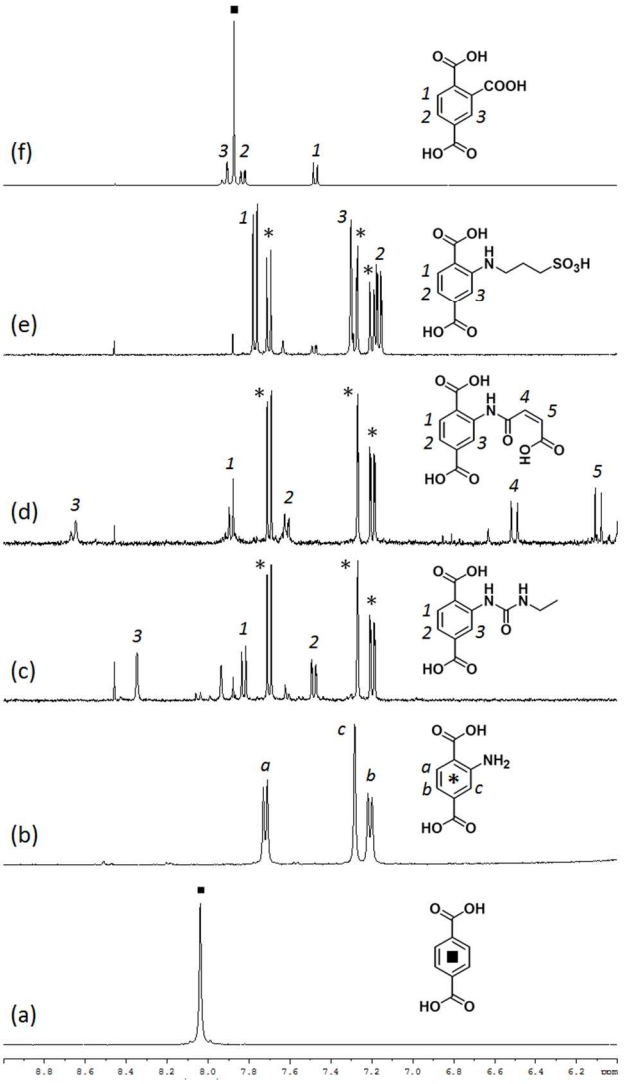

Fig. 2 ^{1}H-NMR spectra measured in NaOD/D_2O for (a) MIL-101 (**1**), (b) MIL-101-NH_2 (**2**), (c) MIL-101-*p*UR2 (**3**), (d) MIL-101-*p*Mal (**4**), (e) MIL-101-*p*3SO_3H (**5**), and (f) MIL-101-*p*COOH (**6b**). Asterisk marks indicate the proton signals of unreacted BDC-NH_2. The linkers must be present in their deprotonated forms in the NMR solutions although their protonated forms are displayed for simplicity.

Water vapour sorption measurements

Prior to measurements, MOF samples were activated under reduced pressure at 160 °C for 6 h. Water adsorption isotherms were measured at 298 K using the standard volumetric procedure on a BELSORP-max instrument (BEL-Japan, INC.). The dead volume of the sample cell was automatically measured using helium gas. Pressure equilibrium points were collected automatically when a pressure change is within 0.5% in 500 s. After each measurement, the weight of the samples was measured by a microbalance. A sorption/desorption cycle took roughly 160 h. The volume (V, cm^3) of adsorbed water at each isotherm point was converted to weight (w, g) according to the embedded equation in the operating software, w = (V/22414) × 18.020.

Results and discussion

MIL-101 (**1**) and MIL-101-NH_2 (**2**) served as precursors for the synthesis of the MIL-101 derivatives as well as reference materials for comparing water adsorption properties. MIL-101-NH_2 (**2**), prepared from MIL-101-NO_2, was partially functionalized by post-synthetic modification to produce MIL-101-*p*UR2 (**3**), MIL-101-*p*Mal (**4**), or MIL-101-*p*3SO_3H (**5**), whereas MIL-101-*p*COOH (**6**) was prepared according to a mixed-linker method. The post-synthetic modification occurs on the BDC benzene ring and the degree of functionalization was monitored by ^{1}H NMR through analysis of 6~9 ppm region of the spectra as shown in Fig. 2. The ratios of linkers incorporated within the structure were estimated based on the values determined by signal integration (Table 1). Accordingly, **3**, **4**, and **5** were shown to contain two distinct linkers within their frameworks (i.e. partial functionalization) with ratios of BDC-NH_2 : BDC-UR2 (**3**), BDC-Mal (**4**), or BDC-3SO_3H (**5**) being 0.66 : 0.34, 0.87 : 0.13, or 0.42 : 0.58, respectively. Similarly for **6**, the ratios of BDC : BDC-COOH were found to be 0.61 : 0.39 and 0.46 : 0.54 for **6a** and **6b**, respectively. The PXRD patterns for all MIL-101 derivatives indicated that the framework structures were maintained after the post-synthetic modification reactions were carried out (Fig. S1). Since it was previously shown that the –NO_2 functionality in MIL-101 retards water uptake (α = 0.45 – 0.5) and reduces overall water uptake capacity,[6a] MIL-101-NO_2 was not further studied in this work.

Nitrogen adsorption isotherms for MIL-101 and its derivatives were measured at 77 K to investigate the influence of the various functionalities on the porosity of MIL-101 (Fig. 3). Pristine MIL-101 displayed a Type-I N_2 adsorption isotherm with a high Brunauer–Emmett–Teller (BET) surface area (3070 $m^2 g^{-1}$), which is

Table 1. Summary of porosity and water adsorption properties of MIL-101 and its derivatives.

MOF	Functional groups in structure (%)		Surface area ($m^2 g^{-1}$)		Pore volume ($cm^3 g^{-1}$)	α[a] (P/P_0)	Water uptake (g g^{-1})			
			BET	Langmuir			P/P_0			
							0.10	0.30	0.40	0.90
1	-H =	100	3070	4550	1.64	0.45	0.08	0.11	0.16	1.29
2	-NH_2 =	100	2890	4110	1.45	0.37	0.02	0.11	0.47	0.81
3	-NH_2 : -UR2 =	66 : 34	1330	1790	0.64	0.50	0.02	0.06	0.10	0.55
4	-NH_2 : -Mal =	87 : 13	1670	2390	0.89	0.40	0.04	0.12	0.34	0.71
5	-NH_2 : -3SO_3H =	42 : 58	1020	1710	0.71	0.36	0.07	0.28	0.43	0.70
6a	-H : -COOH =	61 : 39	2380	3550	1.26	0.39	0.06	0.12	0.55	1.02
6b	-H : -COOH =	46 : 54	2110	3220	1.18	0.39	0.06	0.12	0.51	0.91

[*a*] The relative pressure where the water uptake amount is half of that at P/P_0 = 0.90.

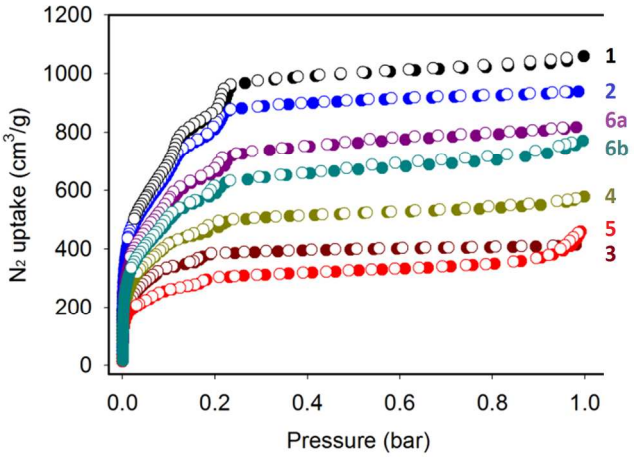

Fig. 3 Nitrogen adsorption (filled circles) and desorption (open circles) isotherms measured at 77K for MIL-101 (**1**), (b) MIL-101-NH_2 (**2**), MIL-101-*p*UR2 (**3**), MIL-101-*p*MaI (**4**), MIL-101-*p*3SO_3H (**5**), and MIL-101-*p*COOH (**6a**, **6b**).

very close to the previously reported value (3124 m^2 g^{-1}).[6a] As expected, all of the MIL-101 derivatives exhibited reduced surface areas in comparison to the pristine, parent MIL-101 as shown in Table 1. The bulkier functional groups with flexible alkyl chains introduced in **3** and **5** presented a greater reduction in the surface area. Contrastingly, the smaller groups introduced in **2** and **6** resulted in less reduction of the surface area. It is reasonable to observe that **6b**, with more –COOH groups in its framework, displays a lower surface area than **6a**. It is worth noting that the isotherms for **3**, **4**, and **5** reduce the characteristic two steps observed in the isotherm of pristine MIL-101. This indicates that the linear functional groups introduced might protrude into the mesopores to reduce the pore sizes. The noticeable increase in adsorption for **5** at higher pressure (> 0.9 bar) is ascribed to the macro pores generated due to particle aggregation. It is likely that the long and flexible alkyl sulfonic acid groups interact with the amine groups exposed on the surfaces of other particles.

Water vapour adsorption/desorption isotherms measured for MIL-101 and its derivatives at 298 K and up to P/P_0 = 1.0 are presented in the ESI (Fig. S2-S8). In all cases, the isotherms display a distinct hysteresis with the magnitudes of deviation between the adsorption and desorption branches being dependent on the functionalities incorporated. For simplicity purposes, only the adsorption branch of the isotherms are displayed in Fig. 4, and the water uptake amounts at P/P_0 = 0.10, 0.30, 0.40 and 0.90 are tabulated and compared along with the α values in Table 1.

The adsorption isotherm of **1** exhibits an "S"-shaped adsorption branch similar to previously reported results and the water uptake capacity of 1.29 g g^{-1} at P/P_0 = 0.9 also lies within the reported values of 1.01, 1.28, and 1.40 g g^{-1}.[3c] The α value of 0.45 for **1** is also similar to previously reported values of 0.46 and 0.50. It is noted that the total uptake capacity is roughly related to the BET surface area and pore volume. The stepwise water uptake observed for MIL-101 is a result of the two different mesoporous cages (2.9 and 3.4 nm in their diameters) that compose the structure.[6a] It is further noted that seemingly continuous isotherms at P/P_0 = 0.4 ~ 0.6 have been observed without the involvement of a distinctive second uptake near P/P_0 = ~ 0.5.[6b,10] Although the reason for this may be attributed to consecutive filling of two hydrophilic pores,[10] it is more likely that this isotherm feature depends on the applied equilibrium conditions used for the measurements. In this work, each isotherm point was recorded when a pressure changed less than 0.5% in 500 s. For the reported isotherms that exhibit distinctive steps for MIL-101 (second step near P/P_0 = ~ 0.5), the measurements were carried out with a smaller pressure change of 0.3 % in 500 s.[6a] Regardless, the isotherm for **1** contains a small step near P/P_0 = 0.45 (Fig. S2).

In contrast to the average α and capacity values for **1**, **2** showed a lower water uptake capacity, 0.81 g g^{-1} at P/P_0 = 0.90, than the two other reported amounts (0.90 and 1.06 g g^{-1} for Cr-MIL-101-NH_2 *a*[6a] and b,[6b] respectively). However, the BET surface area (2890 m^2 g^{-1}) and pore volume (1.45 cm^3/g) of **2** are no less than those reported for Cr-MIL-101-NH_2 *a* (2509 m^2 g^{-1}, 1.27 cm^3/g)[6a] and for Cr-MIL-101-NH_2 *b* (2690 m^2 g^{-1}, 1.6 cm^3/g).[6b] In addition, the α value of **2** (0.45) is slightly larger than the previous results (0.36 and 0.42 for Cr-MIL-101 *a* and *b*, respectively). The isotherm of **2** showed an additional step at P/P_0 = ~ 0.35 not observed in the previous reports, which is difficult to interpret at this moment. Despite the noticeable differences in water adsorption properties of **2** with respect to the previously reported results, the general feature of $–NH_2$ functionalization in MIL-101 has been confirmed again in this work: the main water uptake take places at a lower pressure with a smaller α value than **1**.

When compared to **1**, the functionalized MOFs (**2** to **6**) exhibit pronounced stepwise curves in the water adsorption isotherms. This is in line with previous reports concerning other MIL-101 derivatives functionalized with -NO_2, -NH_2, or -SO_3H groups.[6] The total water uptake values again are roughly related to the BET surface areas and pore volumes. It is observed that the BET surface areas and pore volumes are decreasing in the order of **1** > **2** > **6a** > **6b** > **4** > **3** > **5** (BET surface areas) and **1** > **2** > **6a** > **6b** > **4** > **5** > **3** (pore volumes), while the order of water uptake amounts at P/P_0 = 0.90 was **1** > **6a** > **6b** > **2** > **4** > **5** > **3**. If these values are compared with the appropriate corresponding parent structure, **1** or **2**, better correlations are observed. For the derivatives of **1**, the decrease in BET surface areas and pore volumes (**1** > **6a** > **6b**) is same as the reduction trend for the total water capacities. A similar observation is made for **2** and its derivatives: **2** > **4** > **3** > **5** (BET surface areas) and **2** > **4** > **5** > **3** (pore volumes) vs. **2** > **4** > **5** > **3** (total capacities). Interestingly, the reduction in the total capacities (-32 and -12 % for **3** and **4**, respectively) is sufficiently correlated to the degree of introduced functional groups (34 and 13 % for **3** and **4**, respectively). This reduction in water capacity is attributed to the increase in the sorbent framework weights as a result of the introduced functional groups. In contrast, **5** only exhibited a 14% reduction in its total capacity compared to the 58% successful post-synthetic modification. It is suggested that the –SO_3H group containing more hydrogen bond acceptor atoms is advantageous for attracting more water molecules. In the case of **6**, the 21 and 30% reduction in capacity for **6a** and **6b**, respectively, are also roughly related to the degree of –COOH functionalization (39 and 58% for **6a** and **6b**, respectively). Thus, it is concluded that this functionality is also effective for water adsorption.

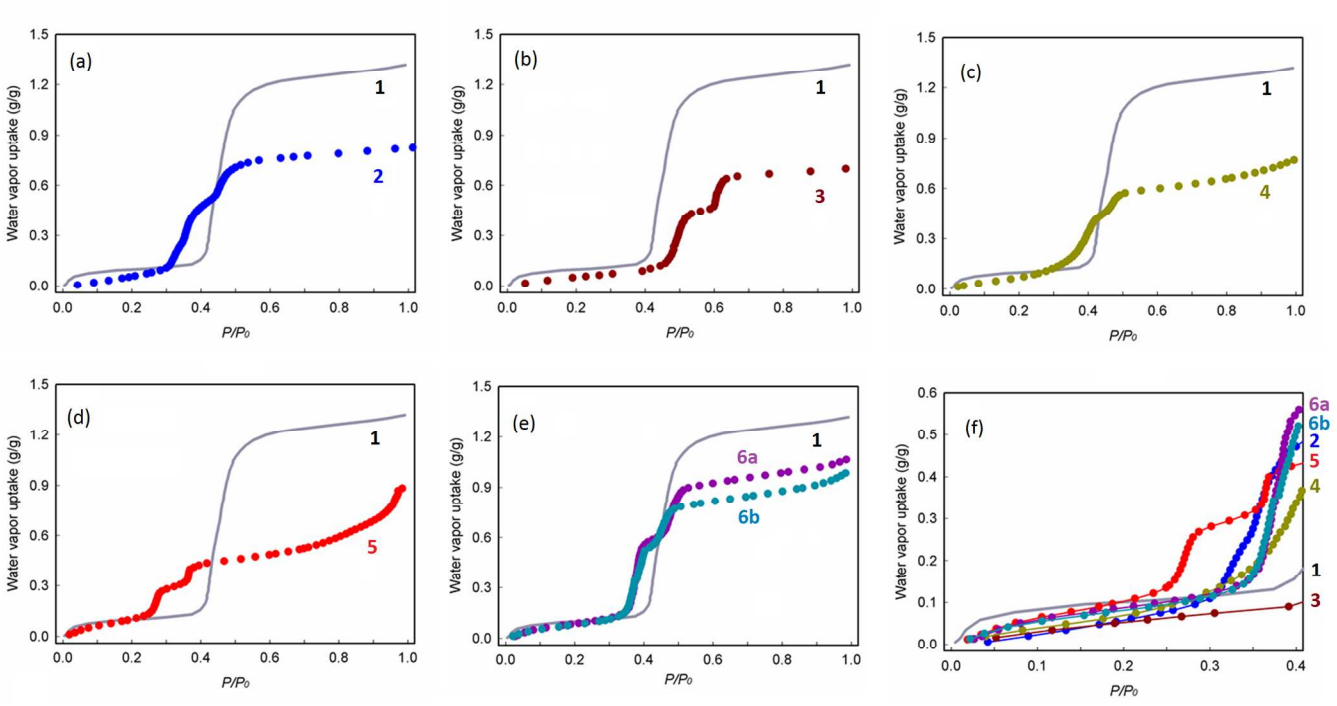

Fig. 4 Water adsorption branch isotherms measured at 298 K for (a) MIL-101-NH_2 (**2**), (b) MIL-101-*p*UR2 (**3**), (c) MIL-101-*p*Mal (**4**), (d) MIL-101-*p*3SO3H (**5**), and (e) MIL-101-*p*COOH (**6a** and **6b**) compared with that of MIL-101 (**1**). (f) Water adsorption isotherms for **1** – **6** displayed together for comparison of the low pressure region. Full adsorption and desorption isotherms are presented in the ESI.

Though it is possible to outline the general changes in the water adsorption properties of these MOFs, the exact contributing influence of the functional groups in the frameworks is difficult to conclusively describe. The reason for this is the fact that there are many possibilities for the relative locations of the functional groups on the faces of ST units (Fig. 1 and 5). For example, **3** could have 4 BDC-NH_2 and 2 BDC-UR2 edges per ST, and the functional groups would be randomly distributed over one ST unit. Thus, it is a significant challenge to determine with high probability the distribution that would occur and exert more positive effect on water adsorption. However, the water adsorption isotherms for the partially functionalized MIL-101 derivatives can provide insights on the functional groups' role in water adsorption.

The derivatives **3**, **4**, and **5** resulted in larger (0.50 for **3** and 0.40 for **4**) or slightly decreased (0.36 for **5**) α values compared to **2** (0.37). It can be said that the introduction of the hydrophilic groups chosen for this study did not improve upon the water uptake affinity of **2**. A structural model of the ST unit in **3** indicated that the terminal ethyl group buries the hydrophilic urea moiety. This means that higher pressures are required for wetting the faces of the ST unit (Fig. 5). For the cases of **4** and **5**, the hydrophobic ethenyl or propyl groups, respectively, are inserted between two hydrophilic sites, leading to a greater separation of the terminal hydrophilic sites from the ST surfaces. Indeed, the hydrophobic spacers are likely to retard the surface coverage of water molecules via hydrogen bonds. This observation is supported by the water adsorption isotherm for MIL-101-SO_3H that does not have alkyl groups. For this MOF, $\alpha = 0.31$, which is much smaller than the 0.36 value found for **5**.[6a] The water uptake capacity at $P/P_0 = 0.4$ for the partially functionalized **3**, **4**, and **5** were shown to be smaller than that of **2**; in particular, **3**, having the terminal ethyl group (-UR2), recorded the lowest capacity. The greater water affinity of the –SO_3H functionality is reflected by the large water uptake amount at low pressure, $P/P_0 = 0.1$. Additionally, the –SO_3H functionality contributes to the largest

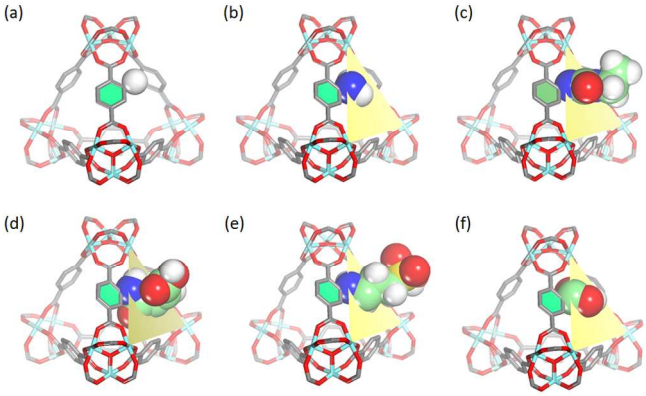

Fig. 5 Comparison of the functional groups and their possible locations on the face of an geometry-optimized ST unit drawn with space-filling models: (a) –H, (b) –NH_2, (c) –UR2, (d) –Mal, (e) –3SO_3H, and (f) –COOH. The STs for MIL-101 and MIL-101-NH_2 are not displayed separately because non-H functional groups give many possible locations and raise complexity. The trigonal faces are defined by thee Cr ions at the ST vertices. All H atoms except for those in the functionalities are omitted, and the oxygen atoms bonded to the Cr centres are also not shown for clarity. The C atoms in the functional groups are highlighted with light green colour.

water uptake value at P/P_0 = 0.3. However, the net water uptake amount of **5** at P/P_0 = 0.10 ~ 0.40 is 0.36 g g^{-1}, which is even smaller than 0.45 g g^{-1} for **2**.

The partial functionalization of MIL-101-NH_2 (**2**) with hydrophilic functionalities that have hydrophobic components proved ineffective for enhancing the water adsorption properties of **2**. Therefore, we sought to investigate the influence of a free –COOH group directly bound to the BDC linker. As the mixed-ligand approach was not applicable for incorporating both –NH_2 and other hydrophilic groups, such as –OH, –SO_3H, –SO_3Na, or –COOH, in the MIL-101 framework (the obtained solids were reported to be amorphous),[15] we decided upon using H_2BDC and $H_2$2-BTC together for the preparation of a new MIL-101 derivative, **6**.

Interestingly, this partial functionalization strategy, with only 39% of –COOH groups incorporated in the **6a** framework, significantly shifted the α values from 0.45 (**1**) to 0.39 (**6a**). Moreover, the water uptake amount at P/P_0 = 0.40 was greatly increased from 0.16 to 0.55 g g^{-1} for **1** and **6a**, respectively. This value was even larger than that (0.47 g g^{-1}) observed for MIL-101-NH_2 (**2**). Furthermore, although the α value of **6a** was slightly larger than that of **2**, the water isotherm of **6a** was steeper than that of **2** (Fig. 4a and 4e).

The partial functionalization with -COOH was further investigated by making **6b**, such that the ratio between BDC and 2-BTC was close to 1 : 1 with 54% incorporation of –COOH groups within the framework. The overall features of the measured isotherm for **6b** were similar to those for **6a** except for a 9% decrease in the total uptake capacity. A notable change is that the height of the second step was reduced in comparison to the first step in the isotherm. This observation is opposite to the general expectation that more hydrophilic groups in the framework improve water adsorption properties over pristine MOFs or at least MIL-101. In other words, partial functionalization with short hydrophilic groups has the potential to be more effective in improving the water adsorption properties of MIL-101 than heavy or full functionalization. This suggestion is supported by the highest water uptake amount by **6a** at P/P_0 = 0.40 among the MOFs studied in this work (Fig. 4f and Table 1). Furthermore, due to its narrow "S"-shaped water adsorption behaviour, the recorded net water uptake amount of **6a** was also the largest value over the range, P/P_0 = 0.10 ~ 0.40. Three cycles of water vapour adsorption measurements resulted in almost same isotherms respectively for both **6a** and **6b**, indicating that the MOFs were not deteriorated during the measurements (Fig. S9). The PXRD patterns obtained before and after the sorption measurements were same, and those for the samples immersed in water for 6 days also were indicative of their water stability (Fig. 10).

Conclusions

The water adsorption properties of MIL-101 or MIL-101-NH_2 have been modified by functionalization of the pristine frameworks with –UR2, –Mal, –3SO_3H, or –COOH groups. Our findings demonstrated that the hydrophilic groups containing hydrophobic components are not effective for improving the water uptake properties. However, by partially functionalizing the framework with short hydrophilic groups (i.e. –COOH), the water adsorption behaviour changes significantly. Furthermore, it was observed that by increasing the incorporation of these hydrophilic groups within the framework, neither water uptake at low pressures nor total uptake capacity was remarkably enhanced. Therefore, it is noted that partial functionalization with short and hydrophilic functional groups is the optimal approach in this study for improving the water adsorption properties of MIL-101 or MIL-101-NH_2 for practical applications. Partial functionalization of the MIL-101 framework affords complex heterogeneity on the super-tetrahedron surfaces. This is primarily a result of the various possibilities of the relative functional group locations. In this regard, a mixed-ligand preparation of MIL-101 derivatives is anticipated to provide even more interesting outcomes.

Acknowledgements

This research was supported by the Energy Efficiency & Resources of the Korea Institute of Energy Technology Evaluation and Planning (KETEP) grant funded by the Korea government Ministry of Knowledge Economy (No. 20122010100120) (J.K.Y.).

Notes and references

[a] Department of Chemistry, Soongsil University, 369 Sangdo-Ro, Dongjak-Gu, Seoul 156-743, Republic of Korea. Fax: +82 2 824 4383, Tel: +82 2 820 0459, E-mail: gllruk123@gmail.com (S.S.), jinkukyang@ssu.ac.kr (J.K.Y.), jaheon@ssu.ac.kr (J.K.)

[b] Center for Molecular and NanoArchitecture, Vietnam National University – Ho Chi Minh City, 721337, Vietnam

† Electronic Supplementary Information (ESI) available: General procedures, PXRD patterns, and full water vapour adsorption/desorption isotherms. See DOI: 10.1039/b000000x/

1 a) P. Guo, A. G. Wong-Foy and A. J. Matzger, *Langmuir*, 2014, **30**, 1921; b) R. Plessius, R. Kromhout, A. L. D. Ramos, M. Ferbinteanu, M. C. Mittelmeijer-Hazeleger, R. Krishna, G. Ronthenberg and S. Tananse, *Chem. Eur. J.*, 2014, **20**, 7922; c) H. Furukawa, F. Gándara, Y.-B. Zhang, J. Jiang, W. L. Queen, M. R. Hudson and O. M. Yaghi, *J. Am. Chem. Soc.*, 2014, **136**, 4369.

2 a) H. Yang, H. Zhu, M. M. R. M. Hendrix, N. J. H. G. M. Lousberg, G. de With, A. C. C. Esteves and J. H. Xin, *Adv. Mater.* 2013, **25**, 1150; b) J. G. Ji, R. Z. Wang and L. X. Li, *Desalination*, 2007, **212**, 176.

3 a) S. K. Henninger, F. Jeremias, H. Kummer and C. Janiak, *Eur. J. Inorg. Chem.* 2012, 2625; b) F. Jeremias, D. Frohlich, C. Janiak and S. K. Henninger, *New J. Chem.*, 2014, **38**, 1846; c) J. Canivet, A. Fateeva, Y. Guo, B. Coasne and D. Farrusseng, *Chem. Soc. Rev.*, 2014, **43**, 5594; d) Y. I. Aristov, *Appl. Therm. Eng.*, 2013, **50**, 1610.

4 S. K. Henninger, F. P. Schmidt and H.-M. Henning, *Appl. Therm. Eng.* 2010, **30**, 1692

5 J. Canivet, J. Bonnefoy, C. Daniel, A. Legrand, B. Coasne and D. Farrusseng, *New J. Chem.*, 2014, **38**, 3102.

6 a) G. Akiyama, R. Matsuda, H. Sato, A. Hori, M. Takata and S. Kitagawa, *Microporous Mesoporous Mater.*, 2010, **157**, 89; b) A.

Khutia, H. U. Rammelberg, T. Schmidt and S. Henninger, *Chem. Mater*., 2013, **25**, 790.

7 a) S.-N. Kim, J. Kim, H.-Y. Kim, H.-Y. Cho and W.-S. Ahn, *Catalysis Today*, 2013, *204*, 85; b) F. Jeremias, V. Lozan, S. K. Henninger and C. Janiak, *Dalton Trans*., 2013, **42**, 15967.

8 a) H. Reinsch, M. A. van der Veen, B. Gil, B. Marszalek, T. Verbiest, D. de Vos and N. Stock, *Chem. Mater*., 2013, **25**, 17; b) M. F. de Lange, C. P. Ottevanger, M. Wiegman, T. J. H. Vlugt and J. Gascon, *CrystEngComm*., DOI: 10.1039/c4ce01073f.

9 G. Ferey, C. Mellot-Draznieks, C. Serre, F. Millange, J. Dutour, S. Surble and I. Margiolaki, *Science*, 2005, **309**, 2040.

10 P. Küsgens, M. Rose, I. Senkovska, H. Fröde, A. Henschel, S. Siegle and S. Kaskel, *Microporous Mesoporous Mater.*, 2009, **120**, 325.

11 J. Ehrenmann, S. K. Henninger and C. Janiak, *Eur. J. Inorg. Chem*., 2011, 471.

12 S. Bernt, V. Guillerm, C. Serre and N. Stock, *Chem. Commun.* 2011, **47**, 2838.

13 S. J. Garibay, Z. Wang, K. K. Tanabe and S. M. Cohen, *Inorg. Chem*., 2009, **48**, 7341.

14 D. Britt, C. Lee, F. J. Uribe-Romo, H. Furukawa and O. M. Yaghi, *Inorg. Chem.* 2010, **49**, 6387.

15 M. Lammert, S. Bernt, F. Vermoortele, D. E. De Vos and N. Stock, *Inorg. Chem.* 2013, *52*, 8521.

16 J. Yang, Q. Zhao, J. Li and J. Dong, *Microporous Mesoporous Mater.*, 2010, **130**, 174.

Graphical Abstract

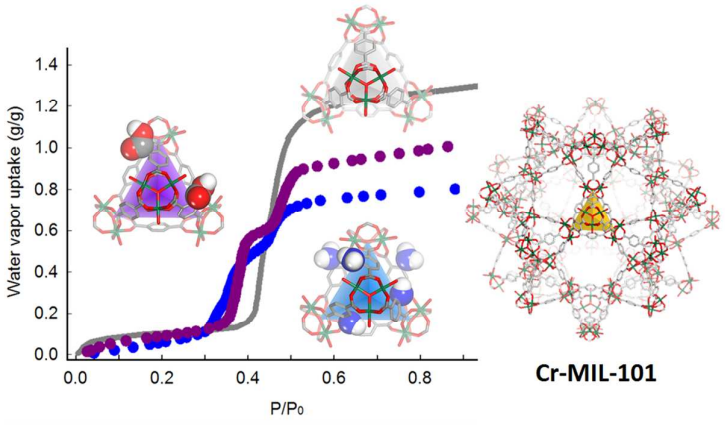

Partial functionalization of the metal–organic framework, MIL-101, with –COOH groups is proven effective for enhancing the water uptake capacity at low pressure.